CO_2-Induced PMMA Swelling and Multiple Thermodynamic Property Analysis Using Sanchez−Lacombe EOS

Dehua Liu, Hongbo Li, Michael S. Noon, and David L. Tomasko*

Department of Chemical and Biomolecular Engineering, The Ohio State University, 140 West 19th Ave, Columbus, Ohio 43210

Received December 25, 2004; Revised Manuscript Received March 21, 2005

ABSTRACT: The Sanchez−Lacombe equation of state (SL EOS) is often used to describe polymer−gas systems because of its inherent ability to hand compressible fluids, but it has rarely been tested for correlating multiple thermodynamic properties of these systems. The real value of an EOS as a process design tool is the ability to describe all thermodynamic properties, not just those it has been fit to. Because of the relatively small amount of data for polymer−gas systems, there is no heuristic to determine which property should be used to fit the EOS to give the best representation of other properties. We test this idea by looking at dilation, solubility and T_g in the CO_2−PMMA system. Although CO_2 sorption phenomena in polymers have been extensively investigated, the study of CO_2-induced polymer dilation is rather limited in comparison. A new experimental technique based on ADSA (axisymmetric drop shape analysis) was developed in this work to measure volumetric properties. The dilation isotherm was measured over temperatures of 40−200 °C and pressures up to 100 bar. The experimental swelling data are then modeled using the SLEOS and the correlated interaction parameter between gas and polymer decreases linearly with temperature within the range 40−160 °C. The applicability of SLEOS to describing thermodynamic behavior of gas−polymer mixture is demonstrated by successfully predicting the CO_2 sorption at 30−60 °C and T_g depression.

Introduction

Environmental and toxicity concerns have been motivating tremendous efforts to develop CO_2-assisted polymer processing operations.[1−4] The resulting products range from foam board insulation and high-impact polymer blends to surface-modified biomedical implants and biological microelectromechanical system (bioMEMs) devices.[1] These applications take advantage of the ability of CO_2 to penetrate into the space between polymer chains and alter the chain mobility and free volume characteristics of the matrix. Such variations in the microenvironment can be detected and evaluated by measurable physical properties, including CO_2 solubility, volumetric expansion, glass transition depression, viscosity, and even interfacial tension. In principle, equipped with information on thermoproperties of the mixture and the corresponding pure component volumetric properties, we are able to completely describe all properties of the gas−polymer binary system with an appropriate equation of state. In practice, CO_2 solubility has been studied most extensively and a number of approaches are available to access this.[5−13] As described in our recent review,[1] the measurement techniques are mainly categorized as the gravimetric and barometric methods, the amount of absorbed gas being indicated by either direct weighing sample or monitoring the pressure drop in the gas phase. At low pressures, the volumetric expansion caused by CO_2 sorption influences the measurement negligibly. However, as the expansion increases, the in situ measurements for the gravimetric method are affected by the buoyancy effect while the reduced CO_2 phase volume must be taken into account to correct the results of the barometric method.

In contrast to the numerous documents on CO_2 sorption, there are relatively few articles investigating the polymer swelling induced by CO_2. This could be mainly ascribed to the changes of sample dimensional integrity during sorption and the difficulties in accurately determining the dimensional variations of the specimen. Current major methods include the following: (1) The first is measuring the one- or two- dimension lengthening of a regular polymer bar or film by methods in refs 7, 11, and 13−16. This methodology is specifically suitable for polymer specimen before evident deformation occurs. Moreover, this approach assumes isotropic swelling in three dimensions and the volumetric dilation is related to the linear one by a cubic equation. As a result, the polymer samples are required to be homogeneous, free of strain and un-oriented to meet the assumptions.[13] (2) The second is in situ monitoring of the position of the interface between CO_2 phase and the polymer liquid.[17] This technique is only valid for polymer melts and requires a clear and/or sharp phase boundary. Meanwhile, meniscus curvature poses a challenge of calculating the volumetric expansion.

In this work, we report new data based on ADSA (axisymmetric drop shape analysis) to measure the volumetric expansion upon CO_2 sorption. The ADSA technique was originally established to measure the surface tension from the shape of an axisymmetric meniscus of a pendant drop. The experimental drop profile is fitted to the theoretical one according to the Bashforth−Adams equation[18] through a nonlinear least-squares algorithm, in which the interfacial tension is fit as the adjustable parameter. The numerical procedure is explained elsewhere.[19] During this optimization process, the volume of drop is calculated simultaneously, which enables the applicability of ADSA to volumetric measurement. Recently, Li[20] employed this method to study the CO_2 effects on the interfacial tension of polymer melts. Wulf et al.[21] have applied this technique

* Corresponding author. Telephone: 614-292-4249. E-mail: tomasko.1@osu.edu.

10.1021/ma047319e CCC: $30.25
Published on Web 04/15/2005

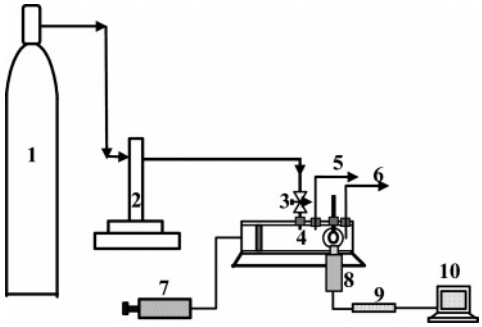

Figure 1. Experimental set up for the polymer swelling measurements under high-pressure CO_2: (1) CO_2 cylinder; (2) syringe pump; (3) valve; (4) high pressure, high-temperature view cell; (5) pressure controller; (6) temperature controller; (7) hydraulic pumps; (8) video camera; (9) VCR; (10) computer.

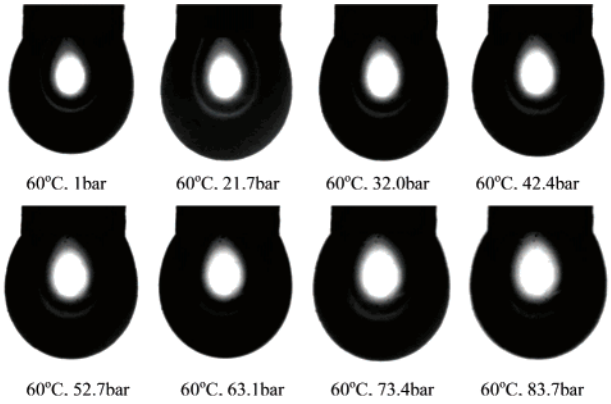

Figure 2. Example images of a PMMA drop in contact with CO_2 at 60 °C and a series of pressures.

to simultaneously measure the polymer density and the surface tension using the sessile/pendant drop method. The densities they obtained using this method compared very well to independently obtained literature *PVT* data.

The volumetric property is an essential aspect of the gas−polymer mixture in equilibrium, from which a thermodynamic model could be established. The real power of an equation of state resides in the capacity for computing multiple properties with all required parameters instead of just correlating the experimental data. However, most of current studies on gas−polymer system focused only on measurement and thermodynamic modeling of one major property, and very few studies were devoted to the description of EOS for multiple properties simultaneously. The solubility and gas-induced glass transition reduction are the other two major aspects that interest people. In the past decades, a number of models have been established to describe the gas−polymer mixture in equilibrium, and the review by Kirby and McHugh is recommended for a comprehensive understanding of the thermodynamic behavior of polymer-CO_2 systems.[22] Among them, the Sanchez−Lacombe equation of state is probably the most widely used model to correlate CO_2 solubility, swelling and shift of the glass transition point.[23−25] As a result, in this work, we not only regressed the interaction parameter between CO_2 and PMMA by fitting the dilation data to SLEOS and investigated its relation to temperature, but also measured the CO_2 solubility and glass transition and then tested the predicting capability of SLEOS model. Consequently, the applicability of SLEOS to gas−polymer system and the best measurable property to fit SLEOS are discussed.

Experimental Section

Materials. The poly(methyl methacrylate) (PMMA) sample (PL150) was obtained from Plaskolite and used without any further treatment. GPC analysis gave the following molecular weight information: $M_w = 80\,200$; $M_n = 41\,700$; $M_z = 116\,400$; polydispersity = 1.92. Carbon dioxide of 99.99% purity was obtained from PRAXAIR.

Swelling Apparatus. The experiments were carried out in custom-designed high-pressure high-temperature view cell, equipped with an adjustable high-resolution CCD camera. The details of this system have been reported elsewhere.[20] The schematic diagram in Figure 1 gives the details of the major components. The system was first purged with CO_2 for a few minutes. The rod with a perfect polymer drop (see below) at the end was delicately inserted into the high pressure and high temperature (HPHT) view cell through a bored-out Swagelok fitting. After the camera was adjusted to produce a good-quality image with sharp drop profile and clear boundary between the rod and solid drop, the system was heated to the desired setting and was followed by introduction of CO_2 into the view cell. An ISCO 500D pump and SENSOTEC pressure gauge were used to control and monitor the CO_2 pressure. The images were continually captured and analyzed to record the entire CO_2 penetration kinetics. When several consecutive measurements yielded a nearly equivalent drop volume, the polymer was considered saturated with CO_2. After the measurement was completed at one pressure, the experiment was then raised to the next higher pressure.

Drop Preparation. A filament of polymer sample (about 3−10 mg, depending on rod diameter) was attached to the smooth polished surface of 1 mm rod end by preheating the rod to a temperature a bit higher than the polymer melting point. The rod with attached polymer piece was placed in a vacuum oven. A total of 1 or 2 days was allowed to remove the possible bubbles inside the drop and form an axis-symmetric shape. Afterward, the oven was cooled to room temperature naturally in order to minimize the moisture contact with external environment. In addition to achieving a perfect symmetric drop, efforts were made to ensure no weight loss and that no polymer adhered to the rod body during drop formation.

Data Acquisition and Image Analysis. The drop image was captured by commercial ATI Multimedia TV program. After improving the image quality with Photoshop 6.0, SigmaScan Pro is able to edge-track the complete drop profile. A Matlab routine was used to read the drop profile and calculate the volume of the drop. The image distance was calibrated by comparing the pixels of the rod to its real diameter.

Results and Discussion

ADSA Technique Analysis. Figure 2 includes the images of PMMA drops taken at 60 °C and different CO_2 pressures. Although there is no significant difference in appearance, the calculated drop volume increases 20% from 1 to 83.7 bar. To improve the sensitivity of the ADSA technique to volume variation, the drop was made as big as possible. However, in the situation of the interfacial tension study, it is highly recommended that the sample mass should be able to display the variations in drop shape resulting from the force balance between interfacial tension and gravity.

In this measurement, a major experimental error comes from the determination of the boundary between polymer and rod bottom surface. To improve the treatment consistency between images, the boundary was distinctly marked during the Photoshop treatment. It was found that the location of the boundary was nearly fixed at constant pressure setting with at most a few pixels of fluctuation. The computation shows that the consequent volume error is within 1%. Moreover, a complete swelling kinetics curve was generated with

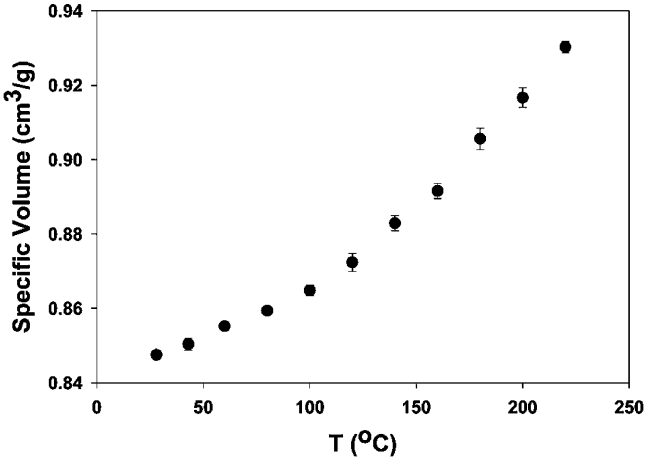

Figure 3. Isobaric temperature vs specific volume of a pure PMMA at ambient pressure.

Table 1. Thermal Expansivity Comparison for PMMA

	β/(cm^3/g·K)		
source	glassy state	liquid State	T_g/°C
this work	0.000242	0.000578	115
literature[26,27]	0.00023	0.00052−0.00055	115 (DSC)

consecutive measurements, from which the true swelling in equilibrium could be identified with strong confidence. Therefore, the experimental errors of swelling data reported in this work are believed to be less than 1% and the error bars are not shown in the related figures.

The isobaric (ambient pressure) density of pure PMMA was first investigated with the purpose of verifying the reliability of the ADSA technique. Figure 3 gives the results averaged from three independent measurements, and the corresponding standard deviations. The obtained data was used to derive the specific SLEOS characteristic parameters of PMMA in this study, which are in good agreement with the literature.[25] The specific thermal expansivity defined as $\beta = (\partial V/\partial T)_P$ is constant over a wider range of temperature than the conventional thermal expansion coefficient, and is used for comparison with literature values along with T_g[26,27] as shown in Table 1. The excellent agreement confirms the applicability of the ADSA technique to monitoring the systems volumetric variations.

Swelling Kinetics and Equilibrium Dilation. In this study, the swelling factor is defined as

$$\mathrm{Sw} = \frac{V_{\mathrm{mix}}}{V_{\mathrm{o}}} \qquad (1)$$

Here V_{mix} and V_0 represent the volume of the gas−polymer mixture at equilibrium and the pure polymer respectively at identical temperatures. As a result, the thermal expansion has been already removed from the swelling expression, and then the gas-induced expansion is specifically addressed.

Figure 4 compares the results in this work with the available literature data at similar temperatures.[7,11] An acceptable agreement between the different data sets is observed, in particular at low pressures. The discernible difference at high pressures could partially be ascribed to the investigation technique. The works of both Wissinger and Kamiya assumed isotropic expansion, and converted the linear one-dimensional expansion to volumetric one by the third-order power law.

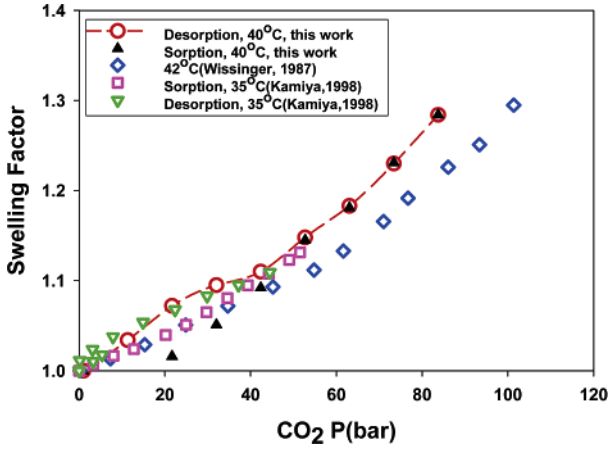

Figure 4. CO_2-induced PMMA dilation at 40 °C.

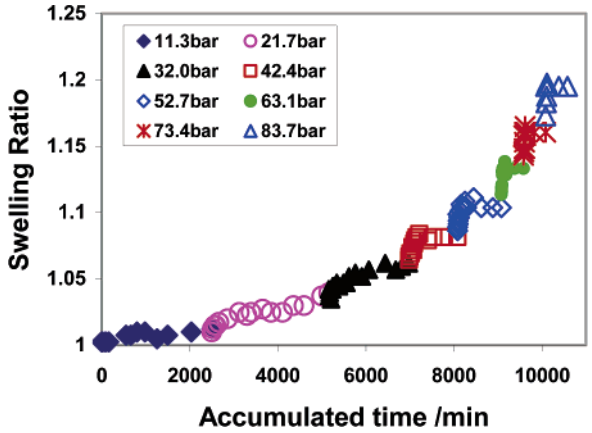

Figure 5. Kinetics of CO_2-induced PMMA swelling behavior at 60 °C and various pressures.

However, as the gas concentration in polymer increases, the plasticization correspondingly becomes more pronounced, which might lead to sample deformation and deviation from isotropic state.

A typical sorption/desorption hysteresis should be observed in the low-pressure part of the isotherm for a glassy polymer, because the initial penetration of CO_2 molecules into the polymer matrix changes the morphological properties of the polymer, which leads to an altered capacity for gas molecules that would manifest itself during a subsequent depressurizing or repressurizing process. The remarkable gap between sorption and desorption that appears in Figure 4 confirms the existence of this hysteresis. The inflection point at which the sorption and desorption data coincides is in the proximity of the glass transition region of the gas−polymer mixture. The hysteresis decreases with increasing experimental temperatures and is hardly observed at high temperatures, confirming its relationship with the glassy state of the polymer.

Figure 5 shows an example of swelling kinetics at 60 °C over a range of pressures. As the pressure increases, the equilibrium time is greatly reduced, ranging from a few days at low pressures down to the order of an hour at high pressures. Similar phenomena were observed for other temperatures lower than the T_g. When the temperature exceeds the normal T_g, the time required to reach saturation is much shorter even at low pressures, mainly on the order of a few hours. The difference in saturation time qualitatively reflects the changes in both the diffusion rate and the concomitant mechanism

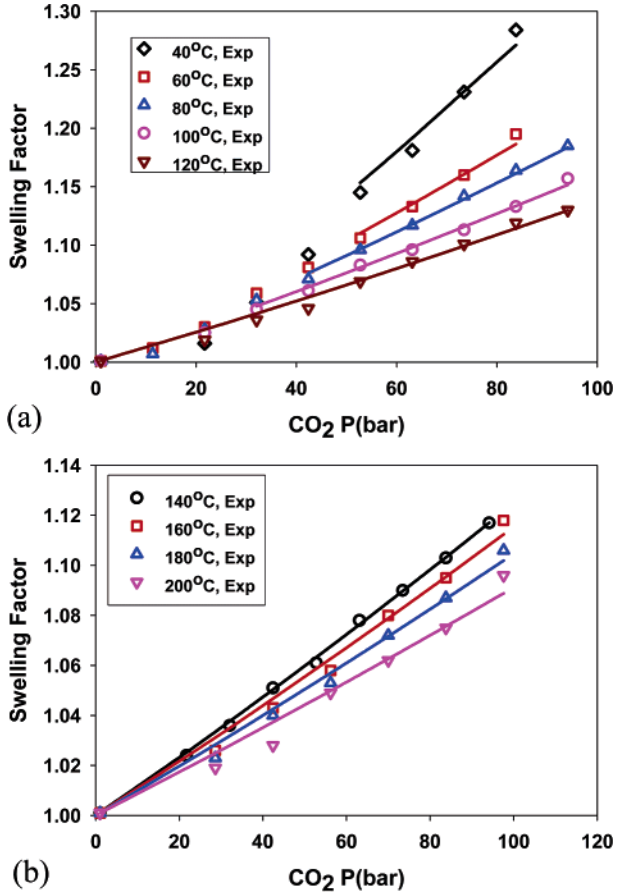

Figure 6. Equilibrium CO_2-induced swelling of PMMA at various temperatures (solid lines represent the SLEOS correlations).

as the polymer transits from the glassy state to the rubbery state. The diffusion rate of gas into a polymer is an area where numerous efforts have been made in the past decades. The physical state, the temperature, and the magnitude of gas pressure simultaneously contribute to the real transmission mechanism. Although, in principle, the recorded kinetic swelling curve contains the essential information on gas diffusion, the lack of explicit diffusion equations for the geometry of an axis-symmetric drop inhibits our further efforts along this direction.

Parts a and b of Figure 6 summarize the extent of PMMA swelling at various temperatures and pressures. The swelling patterns displayed in this figure are not unexpected. In general, the swelling increases with increasing pressure at isothermal conditions, and decreases with the temperature at isobaric conditions. At low temperatures, particularly 40 °C, the region where the state transition occurs is clearly exhibited by a sharper upward trend as the pressure exceeds the point around 57 bar. In contrast, at higher temperatures, the swelling variation as the pressure increases primarily follows a simple linear relationship. The difference in sorption pattern reflects the existence of different sorption mechanisms that is related to the physical state of polymer-CO_2 system. In terms of dual-mode sorption, the sorption in glassy state is comprised of contributions from Langumir's adsorption that is related to unrelaxed free volumes in polymer and dissolution mode that is described by classical linear Henry's law. As the system approaches to the rubbery state, the polymer segments obtain higher mobility and the "freezing-in" unrelaxed free volume holes gradually collapse, which eventually results in a dominant role of dissolution mode. When the system temperature exceeds the normal T_g, the polymer simply exists in a rubbery state regardless of the presence of CO_2, which fits Henry's law well.

SLEOS Modeling of Equilibrium Swelling. The SLEOS[23−25] was employed to correlate the swelling data and explore further the interaction between CO_2 and the polymer matrix. The SLEOS is founded on the lattice fluid model, and its basic form is given by

$$\tilde{\rho}^2 + \tilde{P} + \tilde{T}\left[\ln(1-\tilde{\rho}) + \left(1-\frac{1}{r}\right)\tilde{\rho}\right] = 0 \qquad (2)$$

Here, $\tilde{T}$, $\tilde{P}$, and $\tilde{\rho}$ are the reduced temperature, pressure, and density, respectively. $\boldsymbol{r}$ represents the number of lattices sites occupied by a molecule. The parameters are reduced by characteristic constants as follows:

$$\tilde{T} = T/T^*,\ \tilde{P} = P/P^*,\ \tilde{\rho} = \rho/\rho^*,\ r = \frac{MP^*}{RT^*\rho^*} = \frac{M}{\rho^* v^*} \qquad (3)$$

Here T^*, P^*, ρ^*, and v^* are the characteristic temperature, pressure, density, and volume, respectively. R is the gas constant and M is the molecular weight.

When the SLEOS is applied to the mixture, the same principle is followed with the proper selection of combining rules. Further details of these mixing rules can be found in the original paper of Sanchez[25] and in other SLEOS modeling papers.[28,29] Below are the generalized mixing rules employed in this study:

$$P^* = \sum_i \sum_j \phi_i \phi_j P^*_{ij},\ P^*_{ij} = (1-k_{ij})(P^*_i\, P^*_j)^{0.5} \qquad (4a)$$

$$T^* = P^* \sum_i (\phi_i{}^0 T^*_i/P^*_i),\ 1/r = \sum_i (\phi_i{}^0/r_i{}^0) \qquad (4b)$$

$$\phi_i{}^0 = \frac{\phi_i P^*_i/T^*_i}{\sum_j (\phi_j P^*_j/T^*_j)},\ \phi_i = \frac{w_i/\rho^*_i}{\sum_j (w_j/\rho^*_j)} \qquad (4c)$$

As noted in the above equations, an interaction parameter k_{ij} is introduced to account for the deviation of P^*_{ij} from the geometric mean. This parameter is essential in accurately modeling the mixture behavior, and provides clues on understanding the affinity of gas molecules to the polymer. For modeling a gas−polymer system, the polymer can be assumed to be nonvolatile and insoluble in the gas phase and the value of interest (usually, mass or volumetric fraction of gas in the polymer phase) is computed iteratively until the gas chemical potential in both the gas and polymer phases are equal.

The SLEOS was based on the model of a molecular fluid, in which all r-mers are capable of moving and are in a thermodynamically equilibrium state. Therefore, the regular SLEOS is not valid for describing the glassy state. Although a modified nonequilibrium lattice fluid model has emerged recently to take into consideration the "freezing-in" structure of glassy polymers,[30−32] this work focuses on testing the applicability of SLEOS to describe the equilibrium state of binary mixtures. Meanwhile, the adjustable parameter, k_{ij}, is examined in terms of its relation to the temperature as well. Table 2 lists the characteristic parameters of PMMA and CO_2 used in this work. Since there is more than one set of

Table 2. Sanchez−Lacombe Pure Component Characteristic Parameters

substance	T^*/K	P^*/MPa	ρ^*/(kg/m^3)	MW	ref
CO_2	269.5	720.3	1580	44	8
PMMA	741.38	500.16	1247.9	80 200	this work

Table 3. SLEOS Correlation with Swelling Data

T/°C	k_{ij}	AARD/%
40	−0.0756	4.1
60	−0.0896	4.2
80	−0.1126	6.6
100	−0.1282	3.2
120	−0.1427	6.4
140	−0.1589	1.8
160	−0.1751	7.1
180	−0.1866	6.9
200	−0.1903	12.5

CO_2 SLEOS parameters available in the literature,[8,33,34] we emphasize that the value of the regressed interaction parameter is definitely dependent on the choice of CO_2 parameters. However, calculations convincingly verify that the correlation results with a fitted interaction parameter are independent of parameter set, as are predicted results among solubility, swelling and glass transition temperature (fitting one type of data and predicting the others).

The data fitting was performed through searching for the minimum of the following objective function:

$$\text{obj} = \sum \left(\frac{|\text{Sw}_{\text{fit}} - \text{Sw}_{\text{exp}}|}{\text{Sw}_{\text{exp}}} \right)^2 \tag{5}$$

The correlation quality was evaluated by

$$\text{AARD} = \sum \frac{|\text{Sw}_{\text{fit}} - \text{Sw}_{\text{exp}}|}{\text{Sw}_{\text{exp}}} \times \frac{1}{N} \times 100 \tag{6}$$

Here, N represents the actual number of data used for the correlation. Sw_{exp} is the experimental extent of swelling. Sw_{fit} is the predicted swelling factor, as calculated by the equation with variables obtained from the SLEOS model:

$$\text{Sw}_{\text{fit}} = \frac{\rho_{\text{polymer}}/\rho_{\text{mix}}}{(1 - \text{mf})} \tag{7}$$

Here, ρ_{polymer}, ρ_{mix}, and mf refer to the density of the pure polymer, the gas−polymer mixture and the CO_2 mass fraction in mixture, respectively.

In Figure 6, SLEOS correlations over all studied temperatures are represented by solid lines, which visually demonstrate satisfactory fits. For temperatures lower than normal T_g of polymer, the minimum CO_2 pressure required to induce the plasticization has to be identified. The appropriate range of dilation data to perform the correlation was determined according to the experimental and modeling results of CO_2 plasticization (shown later in Table 4). The obtained interaction parameter and the corresponding AARD are listed in Table 3. Indeed, we found that the correlated k_{ij} is not strongly dependent on the pressure range selected, even at the conditions where the glassy state still holds. However, the estimated fitting errors might be distinctly different when the low-pressure data was incorporated into the correlation.

Currently, there are no conclusive remarks on the relation of this parameter to system variables, such as

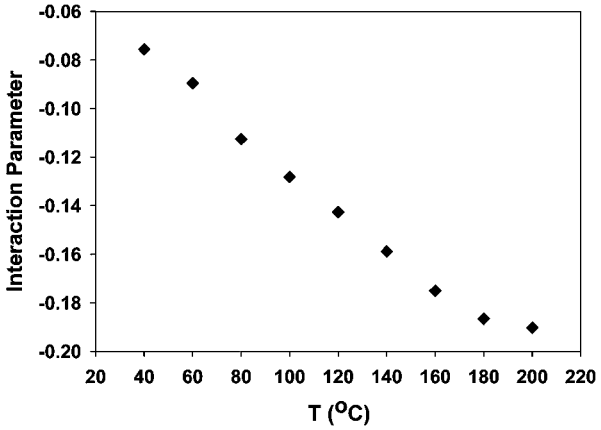

Figure 7. Relationship between the temperature and interaction parameter.

Table 4. Comparison of CO_2 Glass Transition Pressure Determined by Correlation with Constant k_{ij} and Prediction Using Temperature-Dependent k_{ij}'s Obtained from Solubility Data

	P_g/bar	
T/°C	prediction approach	correlation approach
30	63.2	40.5
40	67.2	47.7
50	68.2	54.0
60	65.7	58.3
80	51.1	56.0
100	25.0	32.8

temperature or pressure. In a recent review,[1] Tomasko mentioned no clear trend of the k_{ij} with temperature by compiling values from several sources of PS−CO_2 systems. Sato[8,33,35] derived a correlation between k_{ij}, temperature and concentration based on CO_2 solubility data in PS. Figure 7 clearly illustrates the effects of temperature on the interaction parameter for this system. Here we find the interaction parameter varies in a fairly linear way as a function of temperature. However, when the temperature increases up to 180 or 200 °C, the interaction parameter seems less dependent on the temperature. Meanwhile, as shown in Table 3, the correlation of the data at 200 °C is poorer than other points, which might be due to the less accurate experimental data. It means the variation of interaction parameter in high-temperature range needs to be further verified. A good way to check the validity of the obtained parameters is to predict the sorption isotherm with them, and compare the results with independent experimental data.

When the interaction parameter between gas and polymer at a certain temperature is known, the corresponding property calculation via SLEOS is straightforward. The expression below is derived to calculate the interaction parameter within the range 40−120 °C.

$$k_{ij} = -0.0009T - 0.0406 \tag{8}$$

Here T is the temperature in °C.

In following discussion, at temperatures other than experimental ones, the k_{ij} is calculated by above k_{ij} relation. At the same time, the original correlated k_{ij} is directly used wherever the experimental swelling temperature is involved.

Thermodynamic Property Prediction. (1) Prediction of CO_2−Induced T_g Depression. In gas−polymer binary systems, the glass transition tempera-

ture is usually lower than the T_g of the pure polymer, since the presence of gas molecules increases the free volume and enhances the chain mobility. This effect is directly dependent on gas concentration in the polymer matrix. For a fixed temperature, the pressure at which the polymer transits to the rubbery state is defined as the glass transition pressure, denoted by P_g. Combined with the Gibbs−Di Marzio criterion of the glass transition,[36,37] the SLEOS was reported as being able to predict and correlate the CO_2-induced T_g depression. Further details of this approach can be found elsewhere.[34,38] The key is to find the solution that makes the entropy of the mixture to be equal to zero at the T_g. The entropy is given by

$$-\frac{S}{krN} = (\tilde{v}-1)\ln(1-\tilde{\rho}) + \frac{\ln\tilde{\rho}}{r} + \left(\frac{\phi_1}{r_1}\right)\ln\left(\frac{\phi_1}{r_1}\right) + \left(\frac{\phi_2}{r_2}\right)\ln\left(\frac{\phi_2}{r_2}\right) + 1 + \frac{\ln(2/z)-1}{r} + \left(\frac{\phi_1}{r_1}\right)(r_1-2)\left[\ln(1-f_1) - f_1\frac{\Delta\epsilon_1}{kT}\right] + \left(\frac{\phi_2}{r_2}\right)(r_2-2)\left[\ln(1-f_2) - f_2\frac{\Delta\epsilon_2}{kT}\right] \quad (8)$$

Here, S represents the entropy, ϕ_i, r_i, r, $\tilde{\rho}$, N, and k are defined as previously in the SLEOS section. z is the lattice coordination number, $\Delta\epsilon_i$ is the increase in intramolecular energy that accompanies the "flexing" of a bond in a type i chain molecule. f_i represents the equilibrium number of flexed bonds, given by

$$f_i = \frac{(z-2)\exp(-\Delta\epsilon_i/kT)}{1+(z-2)\exp(-\Delta\epsilon_i/kT)} \quad (9)$$

In this study, the coordination number z follows the same value of 10 employed by Condo.[34] The $\Delta\epsilon$ of a simple small molecule is equal to zero, while the $\Delta\epsilon_2$ of the polymer molecules can be obtained by setting temperature and ϕ_1 equal to normal T_g and 0, respectively, and employing the reduced density of polymer at normal T_g and pressure of 1 atm in above entropy expression.

In current T_g modeling works, the interaction parameter was assumed to be independent of temperature. However, the above k_{ij} discussion already demonstrates k_{ij} is a function of temperature, which implies the inappropriateness of the assumption. Fortunately, the sufficient k_{ij} information over a wide range of temperatures in this work offers an opportunity to test the entropy approach of identifying the transition point of a mixture. Figure 8 shows the effects of k_{ij} on the relation of T_g to P_g, in which most k_{ij}s are just true values at experimental temperatures. It shows the retrograde vitrification is a common phenomenon observed for most interaction parameters studied. Condo[34] originally reported and explained this behavior from the viewpoint of enhanced chain mobility. In other words, the significant dissolution of CO_2 into the polymer at low temperatures can result in similar improved mobility as thermal contribution can. More importantly, it undoubtedly demonstrates the effects of the magnitude of k_{ij} on describing the T_g behavior. As the interaction parameter increases, a higher pressure has to be applied in order to achieve the same T_g. For example, to achieve a T_g of 60 °C for a mixture, the CO_2 pressure needed for the case of $k_{ij} = -0.0756$ is equal to 84.8 bar, while only 38.4 bar is needed when $k_{ij} = -0.1427$. The resulting P_g difference is so large that using a constant

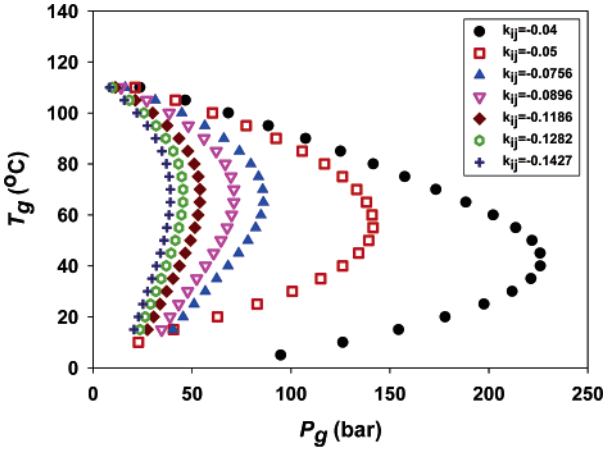

Figure 8. Effects of the interaction parameter on the predicted T_g.

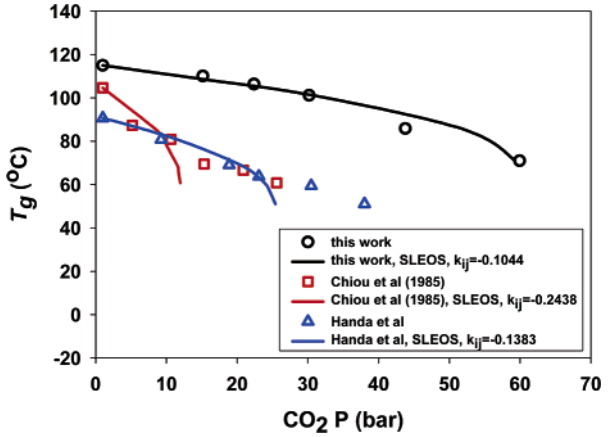

Figure 9. SLEOS correlation to the experimental and literature T_g.

k_{ij} to correlate the T_g data spanning a wide range of temperatures is definitely inappropriate.

The experimental T_g depression data for PMMA was determined utilizing the high-pressure DSC technique using a TA2920 instrument. Figure 9 combines our experimental T_g data and some literature datas for PMMA.[39,40] The solid lines represent the SLEOS correlation made with optimized constant interaction parameters. The values of k_{ij} are shown in the legend of the figure. It is shown that the simple T_g correlation with the SLEOS is acceptable, especially in proximity to normal T_g.

In the meantime, we utilized the obtained k_{ij} relation or real k_{ij} values to predict the transition pressure corresponding to a given temperature with the SLEOS model, as displayed in Figure 10. The correlation result with a constant k_{ij} is also displayed for comparison. In the following discussion, unless stated specifically, the correlation or optimization approach refers to calculation with a constant interaction parameter k_{ij}, whereas prediction refers to results from varied k_{ij}. It is shown that both correlation and prediction approaches give fairly equivalent descriptions of experimental data, particularly in proximity to the normal polymer T_g. The optimized $k_{ij} = -0.1044$ lies approximately amid the real k_{ij} values over the temperature range. Although the combination of the SLEOS with the Gibbs−Di Marzio T_g criterion proves to be a good approach to correlate the available experimental data, the achieved constant interaction parameter, k_{ij} should only be understood

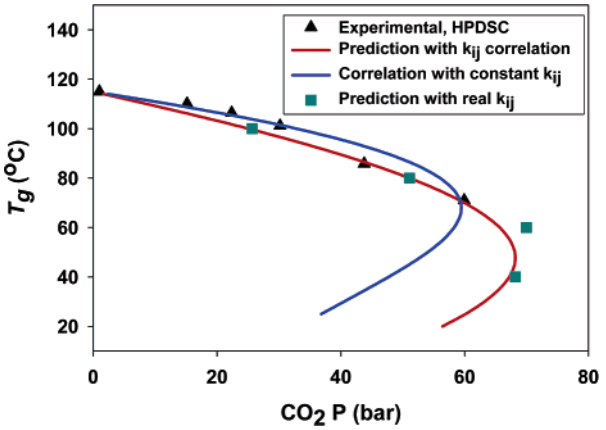

Figure 10. Comparison of the SLEOS correlation with constant interaction parameter and prediction with real interaction parameter.

empirically, not being identical to the regular k_{ij} defined in the SLEOS mixing rules. Further, the pressure at which retro-vitrification begins (maximum pressure on curve in Figure 10) is much lower for the correlated T_g than that predicted using real k_{ij} values. Because of the limitation of high-pressure DSC at the temperatures lower than room temperature, we were unable to provide the experimental data to determine which approach is more appropriate. The glass transition pressures from both approaches for temperatures lower than normal T_g are provided in Table 4 for identifying the proper CO_2 pressure range where the SLEOS holds.

(2) Prediction of CO_2 Solubility. With the k_{ij} information and already determined CO_2 pressure range where the CO_2−PMMA mixture is in the rubbery state, the prediction of CO_2 solubility in PMMA at various temperatures using SLEOS becomes feasible. In general, a CO_2 pressure beyond 65 bar is sufficient to induce plasticization. By comparing the predicted values to experimental ones, the applicability of SLEOS could be further tested. As a result, the CO_2 solubility in PMMA at 30, 40, and 50 °C were determined by the classic gravimetric desorption method, initially developed by Berens et al.[6,41] Briefly, the weight loss of a polymer sample with regular geometry after removing it from the pressure cell was recorded and extrapolated to zero time, which corresponds to the in situ solubility data at saturation. The independence of solubility data from the swelling information is its major advantage.

Parts a−c of Figure 11 illustrate the comparisons at 30, 40, and 50 °C, respectively, in which the data from Wissinger's work[11] are also shown even though the temperature is slightly different. The individual interaction parameters used to predict the isotherm are provided in the legend of the figure, which are either true k_{ij} or calculated by k_{ij} relation. In all three parts of Figure 11, the experimental points lie very near the predicted curve, which demonstrate very good agreement between SLEOS prediction and experiment.

On the other hand, following the same correlation procedure, the interaction parameter was also obtained by fitting the SLEOS to CO_2 sorption data at 30, 40, 50, and 58.8 °C. Table 5 compares the interaction parameters from both dilation and sorption correlations. Both correlations give nearly equivalent results, as indicated by the small deviation (well below 6%). Moreover, the sorption correlation also leads to a linear relationship of the interaction parameter to the temperature, in consistence with the above conclusion from the swelling data.

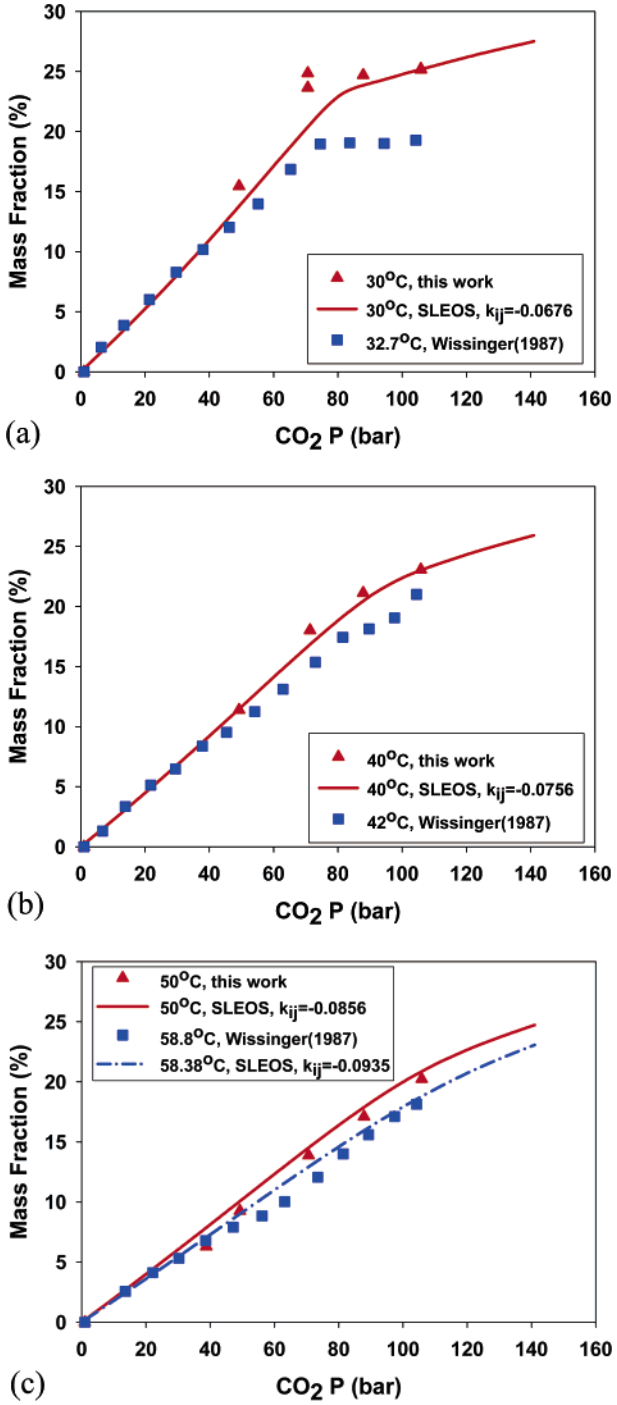

Figure 11. Comparison of experimental and predicted CO_2 solubility by the SLEOS in PMMA.

Table 5. Comparison of Dilation and Sorption SLEOS Correlation

	k_{ij}			
T/°C	dilation	sorption	deviation/%	sorption data source
30	−0.0676	−0.0719	6.36	this work
40	−0.0756	−0.0772	2.12	this work
50	−0.0856	−0.082	4.21	this work
58.8	−0.0935	−0.0892	4.62	11

(3) Comments. The satisfactory agreement between prediction and experiment over both T_g reduction and CO_2 solubility strongly demonstrates that the SLEOS is a robust thermodynamic model for describing physical

properties of a gas−polymer mixture, and capable of performing the task of thermoproperty prediction. The nearly identical interaction parameter regressed from dilation and sorption data not only shows the consistency of the SLEOS, but provides insight into obtaining the necessary parameters to confidently use the SLEOS model for multiple properties. In contrast, the T_g reduction study cannot generate the interaction parameter at a single temperature because only one transition pressure could be determined and the optimization over a single point is definitely not appropriate. While for the dilation and sorption work, there is no evident preference over either of them since both come from SLEOS model simultaneously and lead to nearly identical correlation result. The ADSA technique developed in this study is a versatile method, because it is suitable for a variety of polymers and a broad range of condition, no matter in solid or melt state. The other methods for gas-induced polymer dilation are usually limited by the experimental conditions. Although there are quite a few methods available to measure the CO_2 solubility in polymer, most of them require the input of polymer swelling upon gas sorption to correct the buoyancy effect (gravimetric method) or real gas phase volume (barometric method). However, the correlation comparison in this work shows that the swelling could be confidently obtained by fitting the sorption data into SLEOS model, which then minimizes the necessity of performing dilation measurement.

Conclusions

The pendant drop method and ADSA techniques (Axisymmetric Drop Shape Analysis) were successfully developed to study the swelling behavior of poly(methyl methacrylate) in contact with CO_2. CO_2 was shown to have strong affinity to PMMA and significantly enhance the extent of swelling. As the pressure increases at isothermal conditions, the polymer matrix expands correspondingly. The hydrostatic effect of pressure is not evidently shown within the test pressure range.

The Sanchez−Lacombe equation of state was demonstrated to be a robust thermodynamic model of describing the gas−polymer binary system. With the proper interaction parameter, the SLEOS is capable of correlating and predicting major thermodynamic properties of gas−polymer mixture in rubbery state, namely, gas solubility, gas-induced polymer swelling and glass transition depression. The interaction parameter by fitting the experimental swelling data to SLEOS through a least-squares algorithm was found to be in a negative linear relationship to the temperature within the range 40−160 °C and then decrease at a much slower rate. Furthermore, the predicted CO_2 solubility in PMMA at 30−60 °C coincides very well with independent experimental and literature data. The combination of the SLEOS and the Gibbs−Di Marzio entropy criterion, could either correlate the available T_g depression data with a constant k_{ij} or predict the transition point with known k_{ij} at a specific temperature. Both approaches produce essentially the same level of agreement with experimental results, but they have significant differences in the retro-vitrification region. Either dilation or sorption data could be used to regress the interaction parameter that is required by SLEOS model to predict the thermodynamic properties of the gas−polymer system. The choice depends on the availability of experimental apparatus.

Acknowledgment. Financial support from the National Science Foundation (DMI-0200324) and Owens-Corning Corp. is gratefully acknowledged.

References and Notes

(1) Tomasko, D. L.; Li, H.; Liu, D.; Han, X.; Wingert, M. J.; Lee, L. J.; Koelling, K. W. *Ind. Eng. Chem. Res.* **2003**, *42*, 6431−6456.
(2) Woods, H. M.; Silva, M. M. C. G.; Nouvel, C.; Shakesheff, K. M.; Howdle, S. M. *J. Mater. Chem.* **2004**, *14*, 1663−1678.
(3) Kazarian, S. G. *Polym. Sci., Ser. C* **2000**, *42*, 78−101.
(4) Cooper, A. I. *J. Mater. Chem.* **2000**, *10*, 207−234.
(5) Aubert, J. H. *J. Supercrit. Fluids* **1998**, *11*, 163−172.
(6) Berens, A. R.; Huvard, G. S. In *Supercritical Fluid Science and Technology*; Johnston, K. P., Penninger, J. M. L., Eds.; American Chemical Society: Washington, DC, 1989; p 208.
(7) Kamiya, Y.; Mizoguchi, K.; Terada, K.; Fujiwara, Y.; Wang, J.-S. *Macromolecules* **1998**, *31*, 472−478.
(8) Sato, Y.; Yurugi, M.; Fujiwara, K.; Takishima, S.; Masuoka, H. *Fluid Phase Equilib.* **1996**, *125*, 129−138.
(9) Schnitzler, J. v.; Eggers, R. In *Proceedings of the Fifth Meeting on Supercritical Fluids*; Perrut, P. S., Ed.: Nice, France, 1998; p 93.
(10) Shieh, Y.-T.; Su, J.-H.; Manivannan, G.; Lee, P. H. C.; Sawan, S. P.; Spall, W. D. *J. Appl. Polym. Sci.* **1996**, *59*, 707−717.
(11) Wissinger, R. G.; Paulaitis, M. E. *J. Polym. Sci., Part B: Polym. Phys.* **1987**, *25*, 2497−2510.
(12) Wong, B.; Zhang, Z.; Handa, Y. P. *J. Polym. Sci., Part B: Polym. Phys.* **1998**, *36*, 2025−2032.
(13) Zhang, Y.; Kishore, K.; Gangwani, R. M. L. *J. Supercrit. Fluids* **1997**, *11*, 115−134.
(14) Nikitin, L. N. S.-G.; Ernest, E.; Vinokur, R. A.; Khokhlov, A. R.; Gallyamov, M. O.; Schaumburg, K. *Macromolecules* **2002**, *35*, 934−940.
(15) Shenoy, S. L.; Fujiwara, T.; Wynne, K. J. *Macromolecules* **2003**, *36*, 3380−3385.
(16) Shenoy, S.; Woerdeman, D.; Sebra, R.; Garach-Domech, A.; Wynne, K. J. *Macromol. Rapid Commun.* **2002**, *23*, 1130−1133.
(17) Royer, J. R.; DeSimone, J. M.; Khan, S. A. *Macromolecules* **1999**, *32*, 8965−8973.
(18) Bashforth, S.; Adams, J. C. *An Attempt to Test Capillary Action*; Cambridge University Press and Deighton, Bell and Co.: London, 1882.
(19) Cheng, P.; Li, D.; Boruvka, L.; Rotenberg, Y.; Neumann, A. W. *Colloids Surf.* **1990**, *43*, 151−167.
(20) Li, H.; Lee, L. J.; Tomasko, D. L. *Ind. Eng. Chem. Res.* **2004**, *43*, 509−514.
(21) Wulf, M.; Michel, S.; Grundke, K.; Del Rio, O. I.; Kwok, D. Y.; Neumann, A. W. *J. Colloid Interface Sci.* **1999**, *210*, 172−181.
(22) Kirby, C. F.; Mchugh, M. A. *Chem. Rev.* **1999**, *99*, 565−602.
(23) Sanchez, I. C.; Lacombe, R. H. *J. Phys. Chem.* **1976**, *80*, 2352−2362.
(24) Sanchez, I. C.; Lacombe, R. H. *Polym. Lett. Ed.* **1977**, *15*, 71−75.
(25) Sanchez, I. C.; Lacombe, R. H. *Macromolecules* **1978**, *11*, 1145−1156.
(26) David, D. J.; Misra, A. *Relating Materials Properties to Structure: Handbook and Software for Polymer Calculations and Materials Properties*; Technomic Publishing Co. Lancaster, PA, 1999.
(27) van Krevelen, D. W., Ed. *Properties of Polymers: Their Correlation with Chemical Structure; Their Numerical Estimation and Prediction from Additive Group Contributions, Third Completely Revised Edition*; Elsevier: Amsterdam, The Netherlands, 1997.
(28) Xiong, Y.; Kiran, E. *Polymer* **1994**, *35*, 4408−4415.
(29) Kiran, E.; Xiong, Y.; Zhuang, W. *J. Supercrit. Fluids* **1993**, *6*, 193−203.
(30) Doghieri, F.; Sarti, G. C. *Macromolecules* **1996**, *29*, 7885−7896.
(31) Doghieri, F.; Sarti, G. C. *J. Membr. Sci.* **1998**, *147*, 73−86.
(32) Boudouris, D.; Panayiotou, C. *Macromolecules* **1998**, *31*, 7915−7920.
(33) Sato, Y.; Fujiwara, K.; Takikawa, T.; Sumarno; Takishima, S.; Masuoka, H. *Fluid Phase Equilib.* **1999**, *162*, 261−276.
(34) Condo, P. D.; Sanchez, I. C.; Panayiotou, C. G.; Johnston, K. P. *Macromolecules* **1992**, *25*, 6119.

(35) Sato, Y.; Takikawa, T.; Sorakubo, A.; Takishima, S.; Masuoka, H. *Ind. Eng. Chem. Res.* **2000**, *39*, 4813−4819.
(36) Gibbs, J. H.; DiMarzio, E. A. *J. Chem. Phys.* **1958**, *28*, 373−383.
(37) DiMarzio, E. A.; Gibbs, J. H. *J. Polym. Sci.: Part A* **1963**, *1*, 1417−1428.
(38) Kikic, I.; Vecchione, F.; Alessi, P.; Cortesi, A.; Eva, F.; Elvassore, N. *Ind. Eng. Chem. Res.* **2003**, *42*, 3022−3029.
(39) Chiou, J. S.; Barlow, J. W.; Paul, D. R. *J. Appl. Polym. Sci.* **1985**, *30*, 2633−2642.
(40) Handa, Y. P.; Kruus, P.; O'Neill, M. *J. Polym. Sci., Part B: Polym. Phys.* **1996**, *34*, 2635−2639.
(41) Berens, A. R.; Huvard, G. S.; Korsmeyer, R. W.; Kunig, F. W. *J. Appl. Polym. Sci.* **1992**, *46*, 231−242.

MA047319E